

## General Disclaimer

### One or more of the Following Statements may affect this Document

- This document has been reproduced from the best copy furnished by the organizational source. It is being released in the interest of making available as much information as possible.
- This document may contain data, which exceeds the sheet parameters. It was furnished in this condition by the organizational source and is the best copy available.
- This document may contain tone-on-tone or color graphs, charts and/or pictures, which have been reproduced in black and white.
- This document is paginated as submitted by the original source.
- Portions of this document are not fully legible due to the historical nature of some of the material. However, it is the best reproduction available from the original submission.

**NASA TECHNICAL  
MEMORANDUM**

**NASA TM X-73637**

(NASA-TM-X-73637) APPLICATION OF THE SEM TO  
THE MEASUREMENT OF SOLAR CELL PARAMETERS  
(NASA) 8 p HC A02/MF A01 CSCI 10A

N77-21548

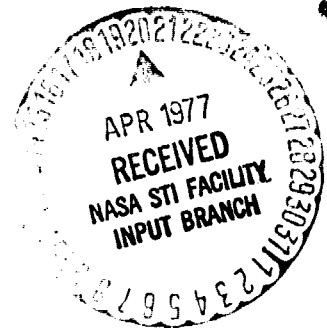
Unclas

G3/44 24351

NASA TM X-73637

**APPLICATION OF THE SEM TO THE MEASUREMENT  
OF SOLAR CELL PARAMETERS**

by Victor G. Weizer and Charles W. Andrews  
Lewis Research Center  
Cleveland, Ohio 44135



TECHNICAL PAPER presented at the  
Tenth Annual Scanning Electron Microscopy Symposium  
sponsored by the Illinois Institute of Technology  
Chicago, Illinois, March 28-April 1, 1977

## APPLICATION OF THE SEM TO THE MEASUREMENT OF SOLAR CELL PARAMETERS

Victor G. Weizer and Charles W. Andrews  
NASA Lewis Research Center  
Cleveland, Ohio 44135

### ABSTRACT

A pair of techniques are described which make use of the SEM to measure, respectively, the minority carrier diffusion length and the metallurgical junction depth in silicon solar cells.

The former technique permits the measurement of the true bulk diffusion length through the application of highly doped field layers to the back surfaces of the cells being investigated. The technique yields an absolute value of the diffusion length from a knowledge of the collected fraction of the injected carriers and the cell thickness.

It is shown that the secondary emission contrast observed in the SEM on a reverse-biased diode can depict the location of the metallurgical junction if the diode has been prepared with the proper beveled geometry. The SEM provides the required contrast and the option of high magnification, permitting the measurement of extremely shallow junction depths, i.e. less than  $0.1 \mu\text{m}$ .

**KEYWORDS:** Silicon Solar Cells, Measurement Techniques, Carrier Diffusion Length, Junction Depth, Electron Beam Induced Current, Surface Field Layers, Depletion Region Edges, Beveled Surface, Semiconductor Devices, Phosphorous Diffusion, Scanning Electron Microscope.

### Introduction

This paper describes two techniques that employ the SEM for the measurement of solar cell parameters which have distinct advantages over other methods. The first is a technique for measuring the minority carrier diffusion length. This technique differs from previous methods in that surface recombination effects are eliminated by the application of highly doped surface field layers, permitting the measurement of the true bulk diffusion length.

The second part of the paper describes a means of measuring shallow junction depths. Here a beveled geometry is employed and it is shown that, under certain conditions, the secondary electron contrast observed in the SEM corresponds to the location of the metallurgical junction. The technique is simple to use and applicable to extremely shallow junctions.

### Diffusion Length Measurement

#### Background

The net distance a minority carrier travels in a semiconductor before being lost through recombination is called the diffusion length,  $L$ . Since the efficiency of a photovoltaic device is very sensitive to  $L$ ,<sup>1</sup> it is important to be able to measure this parameter accurately. This measurement is, however, a difficult one and, while many techniques have been employed, there is a serious lack of agreement among the values obtained by the various methods.

Several investigators have used a technique in which the SEM is employed to generate carriers in a diode sample.<sup>2,3</sup>  $L$  is determined by measuring the short-circuit current,  $I_{sc}$ , of the diode as the SEM beam approaches the collecting junction. The main difficulty with this type of technique is that carrier recombination at the beam entry

ORIGINAL PAGE IS  
OF POOR QUALITY

surface must be accounted for. If this is not done, since  $L$  is a bulk parameter, an erroneous value of  $L$  will result. The problem is most severe for devices such as solar cells which have dimensions comparable with  $L$ . Furthermore, surface inversion effects induced by the SEM beam on P-type material<sup>4</sup> make this technique extremely difficult to apply to P-base devices of moderate to high resistivity, i.e. equal to or greater than 10 ohm-cm. Elimination of these surface effects would greatly simplify the measurement.

The technique to be described here is an SEM technique in which surface effects are eliminated through the use of highly doped surface field layers. The application of such field layers not only reduces surface recombination to negligible values, but also prevents the occurrence of beam induced inversion layer effects. The geometry of silicon solar cells and their large  $L$  values make this an ideal technique for use with them. The first part of this paper will describe the technique and compare the results obtained with it with those obtained using a penetrating radiation (X-ray) technique.

#### Symbols Used in This Paper

$L$	Minority carrier diffusion length.
$I_{sc}$	Solar cell short-circuit current.
$S$	Surface recombination velocity, cm/sec.
$I_{max}$	Carrier generation rate times unit charge.
$s$	Normalized (dimensionless) $S$ ; $s = SL/D_m$ .
$y_1$	$(d - x)/L$ .
$y_2$	$-x/L$ .
$d$	Solar cell thickness.
$x$	Distance from cell junction to carrier injection point.
$D_m$	Minority carrier diffusion coefficient.
$I_B$	SEM incident beam current.
BSF	Back surface field (layer).
$\theta$	Angle between "angle-lapped" surface and original solar cell face.
DRE	Depletion region edge.
$x_j$	Depth of cell junction from front face.
$N_B$	Base dopant concentration (B in Si cell)
$N_0$	Surface concentration during diffusion of phosphorous into solar cell.
$D$	Diffusion coefficient for phosphorous.
$t$	Time of diffusion.
$D_0$	Constant of proportionality, diffusion.
$E$	Activation energy, diffusion of P in Si.
$k$	Boltzmann's constant.
$T$	Absolute temperature, °K.
$C$	Natural log of $(2\sqrt{D_0 t} \text{erf}^{-1}(N_B/N_0))$ .

#### Theory

Let us consider the generation of carriers by the SEM beam at a point inside a silicon solar cell. The cell is assumed to

be a planar device with lateral dimensions much larger than  $L$ . The fraction of generated carriers that is collected by the junction increases with increasing  $L$  and decreases with increasing recombination velocity,  $S$ , at the beam entry surface.<sup>2</sup>

By solving the continuity equation describing point generation of carriers in a planar cell of thickness  $d$ , at a distance  $x$  from the collecting junction, an expression for the collected fraction  $I_{sc}/I_{max}$  is obtained:

$$\frac{I_{sc}}{I_{max}} = \frac{1 + \left(\frac{1-s}{1+s}\right) \exp(-2y_1)}{\exp(-y_2) + \left(\frac{1-s}{1+s}\right) \exp(y_2) \exp(-2y_1)} \quad (1)$$

where  $y_1 = (d-x)/L$ ,  $y_2 = -x/L$ ,  $I_{max}$  is the carrier generation rate times the unit charge,  $s = SL/D_m$  is the normalized value of the rear surface recombination velocity, and  $D_m$  is the minority carrier diffusion coefficient.

For carriers generated just inside the rear surface of the cell, we can set  $x = d$  and obtain the family of curves shown in Fig. 1. Using these curves we can determine  $L$  from the measured value of  $I_{sc}$ , once  $S$  and  $I_{max}$  have been determined.

#### Experimental

Apparatus. A Japan Electron Optics Laboratory JSM-2 SEM was used in these investigations. To permit SEM beam entry into the rear face of the cell, a small (1 mm x 1 mm) window was chemically etched in the aluminum back contact metallization layer, exposing the P<sup>+</sup> silicon layer. The beam current was measured by means of a Faraday cup mounted on the specimen holder.

$I_{sc}/I_{max}$  Determination.  $I_{max}$  can be determined theoretically from the carrier pair production energy (3.63 eV),<sup>5</sup> the incident beam energy (40 keV), the electron backscattering coefficient (0.16),<sup>6</sup> the mean fractional energy loss of the backscattered electrons (0.365),<sup>7</sup> and the incident beam current  $I_B$ . Using these values we have

$$I_{max} = 9.89 \times 10^3 I_B .$$

An experimental determination of  $I_{max}$  can be made by measuring the cell short circuit current as the SEM beam is incident on the front face of the cell where the collection efficiency is expected to approach 100%. The value of  $I_{max}$  measured in this way was found to be less than the theoretical value by approximately 3.5%. The error in the experimental  $I_{max}$  is due mainly to the fact that a portion of the beam induced carriers are produced in and near the "dead" region formed near the surface of the cell during

junction diffusion.<sup>8</sup> Carriers produced within this region are lost due to the extremely short lifetime therein. Fortunately, a similar "dead" region is produced near the rear face of the cell upon application of the field layer.<sup>8</sup> Thus  $I_{sc}$  measured with the SEM beam incident on the rear face of the cell will be subject to approximately the same losses as those in the  $I_{max}$  measurements. Because the ratio,  $I_{sc}/I_{max}$ , is taken, the errors will partially, if not completely, negate one another, providing a reasonably accurate value of the collected fraction.

**Surface Recombination Velocity.** In order to use Fig. 1 to determine L, we must know S. As can be seen from Fig. 1,  $I_{sc}/I_{max}$  decreases rapidly as S increases. Because of noise considerations, the lower the value of S, the greater the ease and accuracy of the measurements. It is desirable, therefore, that the value of S be as low as possible.

While it is known that the application of a highly doped field layer to the surface of a semiconductor effects a reduction in S, uncertainty exists as to the quantitative nature of the reduction. To determine the reduction in S, the following experiment was performed. Special cells were fabricated which contained crescent shaped slots, 1 mm wide and about 1 cm in length, ground in the rear surfaces (Fig. 2). Cell thickness at the bottom of the slot was of the order of 25 microns. After slotting and chemically polishing the surface, the P<sup>+</sup> layer was incorporated by evaporating aluminum onto the rear surface and diffusing at 875°C for 60 minutes. After diffusion the remaining aluminum was removed from the slot and a small adjacent area to permit entry of the electron beam.

Measurements of  $I_{sc}/I_{max}$  were then made as a function of position as the electron beam traversed the length of the slot. Results of the measurement on one of the specially fabricated cells are shown in Fig. 3. The sharp drop in  $I_{sc}/I_{max}$  as the beam enters the slot indicates a higher value of S there than on the flat. This is probably due to residual lattice damage from the slot grinding procedure.

The scatter in the data of Fig. 3 is believed to be due to the presence of tenacious aluminum-silicon alloy particles and other surface irregularities which reduce the magnitude of the beam current that enters the underlying silicon. Thus the true response is best described by the upper envelope of the data.

The best fit of equation (1) to the data along the slotted region is indicated by the solid curve in Fig. 3. The theoretical fit requires a value of 0.315 for s and a

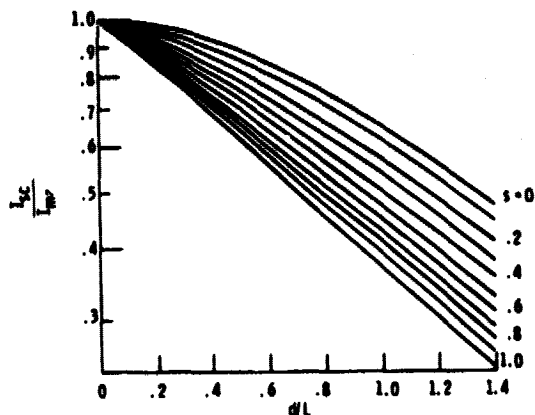


Figure 1. Collected fraction of injected carriers as a function of the ratio  $d/L$ , with  $s(=SL/D_m)$  as a parameter.

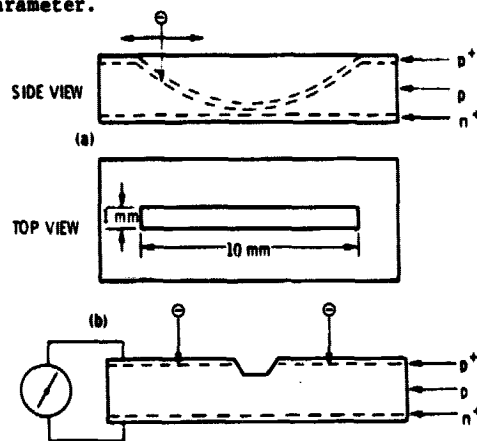


Figure 2. - Schematic diagrams of (a) slotted-back solar cell, and (b) split-back cell.

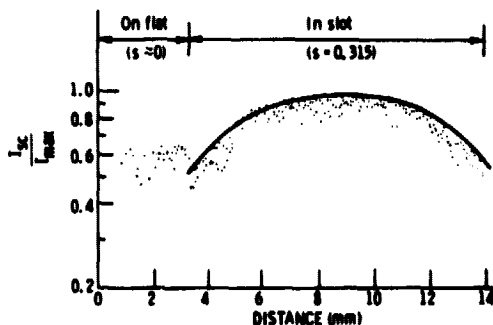


Figure 3. - A plot of the collected fraction of injected carriers as a function of distance across back of cell.

value of 262  $\mu\text{m}$  for L. This value of L can then be used with equation (1) to determine s on the flat, unslotted region. The results of such a calculation indicate that on the flat area,  $s = 0.012$ . Upon translating these numbers to absolute values, one finds recombination velocities of approximately 400 cm/sec in the slot and 15 cm/sec on the flat. The latter value is several orders of

magnitude less than the minority carrier diffusion velocity. This means that, for all practical purposes, the  $P^+$  field layer as described here constitutes a perfectly reflecting barrier to minority carrier transport, effectively preventing recombination at the rear surface of the cell.

**High Injection Level Effects.** No variation was found in the ratio of collected current to beam current over an SEM beam current range from  $5 \times 10^{-12}$  to  $10^{-9}$  amp., indicating that the measurements are free of high injection level effects.

**Low-High Junction Effects.** A low-high junction is formed near the rear face of a cell upon the application of a highly doped field layer.<sup>9</sup> Such a junction could generate a current that would have to be accounted for. A pair of experiments were performed, therefore, to detect possible low-high junction current generation.<sup>10</sup>

The first experiment attempted to measure the photovoltages of isolated  $PP^+$  junctions and the second sought to detect the presence of a low-high junction current component in a split-back cell geometry as shown in Fig. 2. In the latter experiment,  $I_{sc}$  was measured (in the SEM) from one half of the cell while carriers were generated in each half in turn. An increased current when the measured side is illuminated would be an indication of current generation at the  $PP^+$  junction.

Both experiments indicated that for cells with base resistivity of 10 ohm-cm or less,  $PP^+$  current generation is not a concern.<sup>10</sup>

### Results and Discussion

A comparison was made between the results of the SEM measurements on a number of 10 ohm-cm. solar cells with the values of  $L$  determined by a penetrating radiation technique employing X-rays as carrier generators. The details of the X-ray technique, which has been used at this laboratory for several years, are presented elsewhere.<sup>11</sup> A comparison of the results of the SEM measurements with X-ray-technique values of  $L$  is shown in Fig. 4. A good correlation between the results of the two techniques is evident. Agreement is within a multiplicative factor, the SEM lengths being consistently about 1.9 times greater than those determined by the X-ray method. The linearity of the relationship between the results of these two basically different techniques indicates the essential validity of both approaches. A calibration error is indicated, however, in one or both methods. Because the SEM method yields an absolute value of  $L$  from knowledge

of a few easily determined parameters, while the X-ray technique depends upon assumptions as to the carrier generation rate, it is likely that the discrepancy is in the X-ray method.

The performance of an experiment in the X-ray apparatus verified this suspicion.<sup>10</sup> Measurements were made on a number of 10 ohm-cm BSF solar cells both before and after the removal of their field layers. While the results obtained using the original calibration were inconsistent with theoretical expectations, a recalibration of the X-ray apparatus such that it agreed with the SEM results removed all inconsistencies.

The danger of this type of calibration error is present in most of the presently used  $L$  measurement techniques.<sup>12</sup> The main problem is the determination of the carrier generation rate as a function of position within the cell. In this sense the X-ray technique is relatively straightforward in that carriers are generated uniformly throughout the cell and only the absolute rate need be determined. Even here, however, errors were found. Thus there is obvious need for a technique not dependent on external calibration, but depending only on measurement of a few easily determined parameters. The SEM technique described here fills this need.

### Junction Depth Measurement

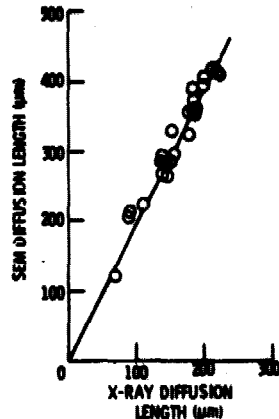
#### Background

A junction depth measurement technique is described which is superior to the angle-lap and stain technique in that it is suitable for use on extremely shallow junctions. We should mention that the elements of this technique already exist in the literature and it is the object of this paper to put them together in print.

**Shallow Junctions.** Creation of the PN junction by solid state diffusion is the most critical step in the production of a solar cell. The efficiency of the cell is controlled by both the perfection of the resulting junction and its depth beneath the surface of the cell.

Solar radiation is very rich in the blue and ultra-violet wavelengths. Unfortunately this light is absorbed very close to the surface of the cell where many of the carriers thus generated are lost by recombination at the surface which essentially competes with the junction for carriers. Thus the closer the junction is to the surface, the greater the percentage of blue-generated carriers that will be collected by the junction and made available to do useful work.

Figure 4 - A comparison of diffusion lengths measured in the SEM with those measured with penetrating radiation.



Moreover, it has been shown that junction perfection itself is improved if shallow diffusions are used.<sup>13</sup> It follows, therefore, that shallow junctions are necessary if greater cell efficiencies are desired.

#### Previous Depth Measurement Techniques.

The most widely used depth measurement technique at the present time is the angle-lap and stain technique.<sup>14,15</sup> Reliance on light microscopy, however, limits the technique to depths greater than 0.5 µm. Furthermore, the technique delineates not the metallurgical junction but the depletion region edge.<sup>14</sup> Unless the junction depth is extracted from the data by some other means, errors up to several hundred percent are possible. Finally, the success of the staining method is quite technique dependent, requiring some "art" for its successful application.

Another method that has been suggested is use of the SEM in the electron beam induced current (EBIC) mode.<sup>16</sup> Here as the SEM beam passes over the junction an EBIC maximum occurs which delineates the junction. The technique has been applied to samples containing very deep junctions and to very short diffusion length samples where the response is highly localized around the junction. EBIC studies at this laboratory on long diffusion length solar cells show an interesting but unusual behaviour. EBIC contrast is observed which appears to be fairly well correlated with the secondary emission contrast (to be discussed here at length). The EBIC contrast mechanism, however, is undoubtedly much more complex and it is far from clear at present whether under all conditions this contrast is located at the junction. If so it would appear feasible to use the EBIC contrast as a depth measurement technique. However, further study is needed to establish the mechanisms operating here.

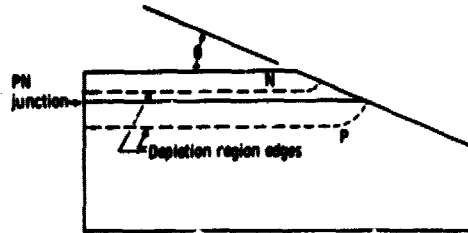


Figure 5 - Schematic diagram of beveled solar cell geometry, showing bending of DRE at bevel surface.

#### The SEM Technique

##### Secondary Electron Emission Contrast.

It is well known that a reverse biased PN junction, observed in the SEM by secondary electron emission, exhibits contrast that is correlated with the P-side DRE.<sup>16,17</sup> This section will show that, for certain cell geometries, this contrast can also indicate the location of the metallurgical junction itself. Therefore, under the proper conditions the SEM contrast can provide a highly accurate, easily used method of determining the location of the metallurgical PN junction, even for junctions as shallow as 0.1 µm.

##### The Effect of Surface Geometry.

A number of investigations have been performed in an attempt to evaluate the effect of surface geometry on electrical breakdown of high voltage diodes.<sup>18,19</sup> A schematic diagram of one of the geometrical configurations considered is shown in Fig. 5. As indicated, a beveled cut was made through the diode intersecting the junction at an angle  $\theta$ . Also shown are the DRE associated with the junction. For a bevel angle of 90° the DRE remain parallel to the junction across the diode. Calculations<sup>18,19</sup> show, however, that as  $\theta$  decreases from 90°, the DRE in the vicinity of the beveled surface no longer remain parallel to the junction plane, but bend, as shown in Fig. 5. Furthermore, as  $\theta$  is reduced to sufficiently small values, the P-side DRE and the junction become coincident at the beveled surface. If a diode with such a small bevel angle were now observed in the SEM under reverse bias, the observed contrast, which designates the intersection of the P-side DRE with the surface, would now also indicate the position of the PN junction. Thus we have a method of measuring the junction depth as long as we can ensure the coincidence of the DRE and the metallurgical junction at the beveled surface.

At first glance the latter condition seems difficult to satisfy since the critical bevel angle depends upon device specifications such as the junction depth and the base resistivity.<sup>18,19</sup> Fortunately it is not necessary to repeat the laborious analysis for every set of diode conditions. Bakowski<sup>19</sup> showed that if the geometry of the diode is such that the DRE coincide with the junction

at the surface, then application of a bias voltage will have no effect on the position of the DRE. This behaviour is in contrast to that of a normally configured diode where the application of a reverse bias causes significant expansion of the depleted region.<sup>20</sup>

We can conclude, therefore, that in a properly beveled sample, if the DRE is invariant with reverse bias, then the DRE and the junction coincide and the contrast observed in the SEM corresponds to the location of the metallurgical PN junction.

This test was applied to a group of solar cells with shallow junctions (less than 0.5  $\mu\text{m}$ ; base resistivity = 10 ohm-cm) which were angle lapped at 2° and viewed in the SEM. Negligible expansion of the depletion region was observed upon application of a bias. We can conclude, therefore, that for 10 ohm-cm, shallow junction solar cells, lapped at 2°, the DRE is effectively pinned at the metallurgical junction. Thus the observed contrast indicates the location of the junction.

### Results - Phosphorous Diffusion

For phosphorous diffusion in silicon the junction depth,  $x_j$ , can be related to the base doping concentration,  $N_B$ , the phosphorous surface concentration,  $N_0$ , the diffusion coefficient,  $D$ , and the diffusion time,  $t$ , by the relation

$$x_j = 2\sqrt{Dt} \operatorname{erfc}^{-1}(N_B/N_0) \quad (2)$$

The diffusion coefficient,  $D$ , is given by the expression

$$D = D_0 \exp(-E/kT)$$

where  $E$  is the activation energy for diffusion,  $D_0$  is a constant,  $k$  is Boltzmann's constant, and  $T$  is the absolute temperature, °K.

Since  $\operatorname{erfc}^{-1}(N_B/N_0)$  is essentially independent of temperature over the range of interest here, equation (2) can be rearranged taking natural logs of both sides, to give

$$\ln(x_j) = -(E/kT) + C \quad (3)$$

where  $C = \ln(2\sqrt{D_0 t} \operatorname{erfc}^{-1}(N_B/N_0))$ . If now the log of the measured junction depth is plotted against the reciprocal temperature according to equation (3), the slope of the resulting plot should yield the activation energy  $E$ , and the intercept should give the diffusion constant  $D_0$ .

A series of phosphorous diffusions were carried out under conditions which would produce junction depths from several microns to approximately 0.1  $\mu\text{m}$ . The diffusions were performed by the open tube technique with  $\text{POCl}_3$  as the phosphorous source and nitrogen

as the carrier gas.

A plot of  $\log(x_j)$  vs. reciprocal temperature for a number of 30 minute diffusions is given in Fig. 6, from which we find that

$$D = 7.35 \times 10^{-3} e^{-(2.5/kT)} \text{ cm}^2/\text{sec.} \quad (4)$$

This value is in agreement with the results obtained by Mackintosh.<sup>21</sup> However, because the angle-lap and stain technique was used, Mackintosh was limited to the measurement of junction depths greater than 0.5  $\mu\text{m}$ . The data presented here extend the measurement range another order of magnitude to depths less than 0.1  $\mu\text{m}$ .

A plot of the measured junction depth vs.  $\sqrt{Dt}$  should, according to equation (2), be linear through the origin with slope of  $2\operatorname{erfc}^{-1}(N_B/N_0)$ . Use of this format would permit the comparison of data taken on shallow junctions diffused at many temperatures and times. Such a plot is given in Fig. 7 where the solid curve depicts the expected behaviour according to equations (2) and (4). The shallow junction data show excellent agreement with the predicted curve even for the shallowest junction considered.

It appears, therefore, on the basis of this close agreement, that the present technique offers the advantages of simplicity and accuracy to the measurement of even extremely shallow junction depths.

### Summary

The preceding results can be summarized as follows:

1. Values of bulk solar cell diffusion length are obtained from a knowledge of cell thickness and the collected fraction of the injected carrier flux. Close agreement is found between this technique and a penetrating radiation technique.
2. The technique is based on the reduction of the cell rear surface recombination velocity by addition of highly doped field layers.
3. A junction depth measurement technique has been described which makes use of the secondary electron contrast in the SEM to delineate the metallurgical PN junction in angle-lapped silicon solar cells.
4. The advantages of this technique are (a) Simplicity of operation, and (b) High resolution due to the high magnification capability of the SEM. Accurate measurement of junction depths of less than 0.1  $\mu\text{m}$  has been demonstrated.

### References

1. Godlewski, M.P.; Barsons, C.R.; and Brandhorst, H.W.: "Low-High Junction Theory



Applied to Solar Cells". NASA TM X-71492, 1975.

2. Hackett, W.H.: "Electron Excited Minority Carrier Diffusion Profiles in Semiconductors". J. Appl. Phys., 43, 1972, 1649-54.
3. Zimmerman, W.: "Measurement of Spatial Variation of the Carrier Lifetimes in Silicon Power Devices". Phys. Stat. Sol., 12, 1972, 671-78.
4. Green, D.; Sandor, J.E.; O'Keefe, T.W.; and Matta, R.K.: "Reversible Changes in Transistor Characteristics Caused by Scanning Electron Microscope Examination". Appl. Phys. Lett., 6, 1965, 3-4.
5. Fiebiger, J.R.; and Muller, R.S.: "Pair-Production Energies in Silicon and Germanium Bombarded with Low-Energy Electrons". J. Appl. Phys., 43, 1972, 3202-07.
6. Bishop, H.E.: Ph.D. Dissertations, Cambridge (England), 1966.
7. Thornton, P.R.: Scanning Electron Microscopy. Chapman & Hall, London, 1967, 91.
8. Guldberg, J.; and Shroder, D.K.: "Theoretical and Experimental Gain of Electron Excited Silicon Targets". IEEE Trans. Electron. Devices, ED-18, 1971, 1029-1035.
9. Lade, R.W.; and Jordan, A.G.: "On the Static Characteristics of High-Low Junction Devices". J. Electro. Control, 13, 1962, 23-34.
10. Weizer, V.G.: "Diffusion Length Measurement Using the Scanning Electron Microscope". Eleventh IEEE Photovoltaic Specialists Conference, Scottsdale, Arizona, May 1975, 67-71.
11. Lamneck, J.H., Jr.: "Diffusion Lengths in Silicon Obtained by an X-ray Method". NASA TM X-1894, 1969.
12. Reynolds, J.H.; Muelenberg, A: "Measurement of Diffusion Lengths in Solar Cells". J. Appl. Phys., 45, 1974, 2582-2592.
13. Lindmeyer, J.; and Allison, J.F.: "The Violet Cell: An Improved Silicon Solar Cell". Comsat Tech. Rev., 3, 1973, 1-22.
14. Burger, R.M.; and Donovan, R.P.: Fundamentals of Silicon Integrated Device Technology. Prentice Hall, 1967, Chap. 6 & 7.
15. "Test for Thickness of Epitaxial or Diffused Layers in Silicon by the Angle Lapping and Staining Technique". Annual Book of ASTM Standards, Part 43, Am. Soc. Test. Mater., 1976, 468-471.
16. See reference 7 (above), 279-297.
17. MacDonald, N.C.; and Everhart, T.E.: "Direct Measurement of the Depletion Layer Width Variation vs. Applied Bias for a PN Junction". Appl. Phys. Lett., 7, 1965, 267-269.
18. Davies, R.L.; and Gentry, F.E.: "Control of Electric Field at the Surface of PN Junctions". IEEE Trans. Electron. Devices, ED-11, 1964, 313-323.
19. Bakowski, M.; and Lundstrom, K.I.: "Depletion Layer Characteristics at the Surface of Beveled High-Voltage PN Junctions". IEEE Trans. Electron. Devices, ED-20, 1973,

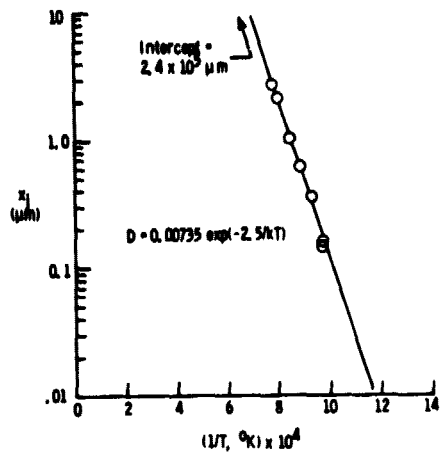


Figure 6. - Logarithm of junction depth plotted as a function of reciprocal of absolute temperature for 30-minute diffusions of phosphorous into 10 ohm-cm silicon.

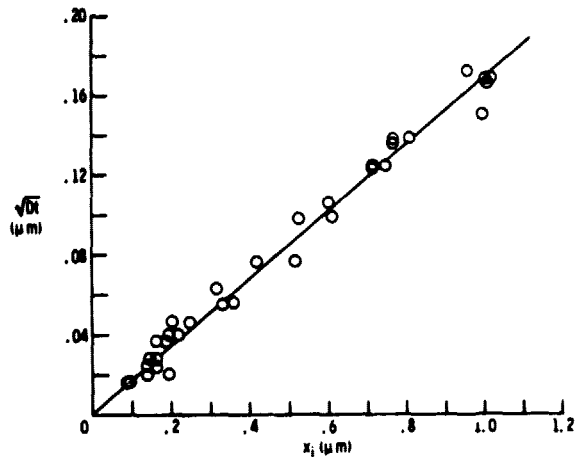


Figure 7. - A plot of  $\sqrt{D}$  against junction depth for several temperatures and times of diffusion of phosphorous into 10 ohm-cm silicon.

550-563.

20. Lindmeyer, J.; and Wrigley, C.Y.: Fundamentals of Semiconductor Devices. Van Nostrand, New York, 1965, Chap. 2.
21. Mackintosh, I.M.: "The Diffusion of Phosphorous in Silicon". J. Electrochem. Soc., 109, 1962, 392-401.